Data-insufficiency prediction for reconstruction in an interior-like problem

Tao Sun, Rolf Clackdoyle, Roger Fulton, Johan Nuyts

***Abstract*–** Previously, we have developed a method to quantify sampling incompleteness for motion-corrected helical CT. The so-called Tuy value was proposed as a measure quantifying the degree to which Tuy's completeness condition is violated in each voxel. In this work, we studied an interior-like problem created by synthesized motion in motion-corrected helical CT. In this interior-like problem which is similar to 2D interior problem, the solution of reconstruction was not unique. One explanation is the incomplete sampling near one position can create artefacts that can even extend to a region where the sampling is complete. However, if some intensities were known inside the interior region, the solution was unique. The results corresponded to the classical theory. We conclude the Tuy map cannot be used to predict the exact reconstruction inside the interior region of such interior-like problem.

I. Introduction

Previously, we have developed a method to quantify sampling incompleteness for motion-corrected helical CT, as a predictor of reconstruction accuracy [1]. The conclusion from that experimental work was, if the Tuy value is very low everywhere, then exact reconstruction is possible (i.e. the reconstruction problem appears to have a unique and stable solution). In contrast, a region of high Tuy values indicates a risk of artefacts there, due to data-insufficiency. However, for the situation of some region of very low Tuy values and other regions of high Tuy values, we cannot conclude that the reconstruction will be unique in the region of low Tuy values. To examine the effectiveness of the proposed Tuy map in such case, in this work, we study an interior-like problem created by synthesized motion in motion-corrected helical CT.

In the 2D interior problem, all projections are truncated transaxially on both sides. Furthermore, for the pixels inside the interior region all projection lines are still available, whereas for the surrounding pixels, some lines are lost due to the truncation. Since the Tuy values will be zero inside the interior region and higher than zero in the surrounding region, this kind of problem is relevant when evaluating our approach. For interior projection data, it is known that the solution is not unique inside the interior region. The reconstructed image may suffer from a DC-shift and low frequency artefacts in the interior region [2]. However, the 2D solution is unique if the interior region extends beyond the support of the object [3], or if the intensities of a small subregion located inside the interior region are known *a priori* [4]–[6].

To examine the effectiveness of the proposed Tuy map on a 3D interior problem, we studied an interior-like problem from a motion-corrected helical CT orbit. The motion was designed such that the local Tuy condition was satisfied within the ROI, but not in the volume surrounding that ROI. Such an interior region could easily be created by reducing the number of detector elements per detector ring. However, a specially-designed motion can also induce such an interior region, if the outer parts of the object occasionally move out of the FOV during the scan. The created data truncation has some similarity to that of the classical 2D interior problem. We then checked how the reconstruction of the interior region was affected by the incomplete sampling in the surrounding structures. The hypothesis was that in this situation, the interior region of the object cannot be exactly reconstructed, unless the interior region extends beyond the support of the object [3]. Note that this is not a straightforward extension of the 2D interior problem to 3D, because in our 3D problem, the low Tuy value volume is only surrounded transaxially by high Tuy values, not axially.

II. Methods

A. Local Tuy condition

The computation of the voxel-based Tuy value can be divided into 3 steps, which are: 1. find all measured projection lines passing through current voxel; 2. find all unit normal vectors representing planes through the voxel, by uniformly sampling a unit hemisphere; 3. compute for each plane the dot product between the normal and all projection lines to find the smallest dot product (in absolute value) for each plane. The Tuy value for the current voxel is the maximum of these smallest dot products over all planes. We call the resulting image the Tuy map. Its values range from 0 to 1, where high values indicate data-insufficiency. Exact stable reconstruction is not possible where the Tuy map contains high values. More details about how to calculate Tuy map can be found in [1].

Manuscript received November 23, 2015. This work was supported in part by grant IWT 130065 of the Flemish agency for Innovation by Science and Technology and by National Health and Medical Research Council Project Grant 632677.

T. Sun and J. Nuyts is with KU Leuven, Department of Imaging and Pathology, Nuclear Medicine and Molecular imaging, B-3000 Leuven, Belgium.

R. Clackdoyle is with Laboratorie Hubert Curien, CNRS and Universite Jean Monnet, France.

R. Fulton is with the Faculty of Health Sciences, University of Sydney, and the Department of Medical Physics, Westmead Hospital, Westmead, Australia.

B. Scanner geometries and simulations

Helical scans were all simulated for the geometry of the Siemens Sensation 16 CT scanner (Siemens Medical Solutions USA, Inc., Malvern, PA). The settings of the parameters were: 16 slices, detector length 672×1.40803 mm, 300 angles per rotation , pitch 1.0, collimation 16×1.5 mm.

We introduced a geometric mismatch with the forward model used by the image reconstruction, by upsampling both the object and the detector by a factor of 2 in all directions when generating the projections. We assumed uniform blank scans, monochromatic radiation and ignored scatter in all simulations. When motion was present, the motion was simulated by applying the inverse motion to the CT-detector gantry for each individual view (as was also done for the reconstruction, see Section II.E).

C. Phantom

Two phantoms were used in this study: (1) A phantom consisting of uniform ellipsoids, inspired by the Shepp-Logan phantom, was created. Its size was 160×160×200 with voxel size of 1×1×1 mm^3; (2) By setting half of the phantom in (1) to zero, the second phantom, shown in figure 2, was obtained.

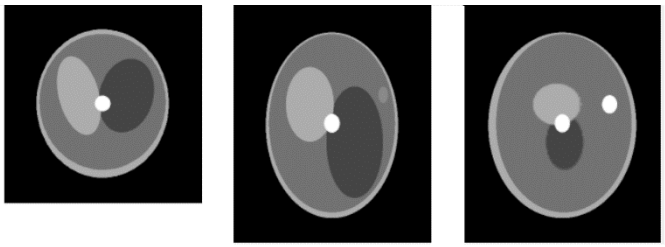

Figure 1 The Shepp-Logan phantom used in simulation (position 80,80,100). The size of the big ellipsoid is 128×128×160 mm. The maximum attenuation was set to 0.04 mm^{-1} .

Figure 2 The half phantom set half of the phantom in figure 1 to zero. The maximum attenuation was set to 0.04 mm^{-1} .

D. Synthesized Motion

We designed a motion to create a pattern of truncation in the projections that would be similar to the situation of the 2D interior problem. For each CT projection view, the object was rotated by a constant angle of 0.3 π about an axis located inside the transaxial plane and perpendicular to both the rotation axis of the scanner and to the line connecting the source and the center of the detector array (figure 3). With such motion, there was always part of the outer object moving out of the FOV during the scan. The motion was large enough to create a pattern of motion-induced data truncation that swept over the exterior region, as the source-detector pair moved in a spiral fashion. The designed motion ensured all outer parts of the object would be outside the FOV for some projection views, while the inner parts of the object always stayed within the FOV.

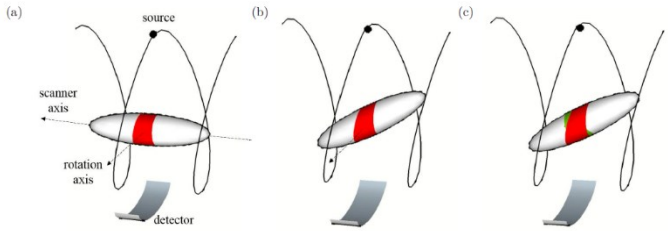

Figure 3 (a) Red region is inside the FOV in current view, (b) after rotation of the object, (c) green region stays out of FOV (axial truncation) after in-view rotation.

E. Reconstruction with motion correction

In the presence of motion, the helical CT orbit is distorted into an effective orbit with arbitrary shape. As shown in [7], an arbitrary effective orbit presents challenges for analytical reconstruction, which can be overcome using an iterative reconstruction algorithm. In the present work, we used the Maximum Likelihood Expectation Maximization (MLEM) reconstruction algorithm [8].

Instead of moving the reconstruction image, rigid motion correction was done by considering a coordinate system fixed to the object and incorporating the motion (now associated to the source-detector pair) into the system matrix. This corresponds to an arbitrary 3-dimensional (3D) motion of the virtual gantry around the object being scanned.

For all static and non-static reconstructions, the voxel size was 1×1×1 mm^3. The ordered subsets technique was adopted to speed up the convergence of the iterative reconstructions [9]. Fifty iterations and 20 subsets were used in all reconstructions to guarantee good convergence of the reconstruction. All projectors/backprojectors were implemented using the distance-driven approach [10]. The reconstructions were used to verify the Tuy map calculated in II.A.

Applying the MLEM algorithm to log-converted transmission data is effective but results in sub-optimal noise characteristics, which can be avoided by using dedicated ML-algorithms for transmission tomography. Noise is not considered in this paper, but we verified that very similar results are obtained with the Maximum Likelihood Transmission Reconstruction algorithm (MLTR) [11], [12]. In both MLEM and MLTR, a non-negativity constraint is applied to the reconstructed image values. With this constraint, zero attenuation along a projection line can only be achieved if all attenuation values along the line are zero. As a result, the reconstructed background values outside the convex hull of the object quickly converge to zero for both algorithms, yielding an exact reconstruction or the background outside the convex hull.

III. Simulations and Results

As described in II. D, we have created interior-like problems both from a synthesized motion, and transaxial detector

reduction in a helical CT scan. The Tuy map was computed to confirm the creation of a 3D interior low Tuy value region, surrounded by higher Tuy values.

As discussed in last Section, we expected the reconstructions to suffer from a DC-shift and/or low frequency artefacts inside the interior region. In a second simulation, the simulation was repeated but now using the half phantom of figure 2 instead of the full Shepp-Logan phantom. With this phantom, the interior region extended beyond the support of the object. As discussed in II.E, this was expected to eliminate the non-uniqueness of the solution inside the region.

A. Data truncation from motion

Figure 4(a) shows the Tuy map for the motion-corrected scan. Near the center of the object, the motion-corrected CT orbit produced a central low Tuy value region transaxially, surrounded by high Tuy values. The high Tuy values indicate the incomplete sampling due to the motion.

We started the reconstruction from a uniform image. The reconstruction converged to an under-estimated solution in the interior region (figure 6a-1st column). To check the uniqueness of this solution, we started another reconstruction from a different image (figure 5a), which was a reference image reconstructed from motion-free projections of the Shepp-Logan phantom. The reconstruction starting from the reference image converged to a solution (figure 6a-2nd column) very close to that starting reference image. A third reconstruction was initialized with a linear combination of previous two solutions. The reconstructed image (not shown here) remained essentially unchanged after several updates, confirming that the problem has multiple solutions. Consequently, the reconstruction problem does not have a unique solution in the interior region of low Tuy values. Therefore, in the interior-like problem one cannot conclude that a local low Tuy value region always indicates that that region can be reconstructed exactly.

Then the half phantom in figure 2 was used and the simulations were repeated for this new object. As initial images we used a uniform image and the reference image of figure 5b. In this case for both initial images, the reconstruction of the interior region converged to the same solution (figure 6a-3rd and 4th columns). By setting half the phantom to zero, the interior region extended beyond the support of the object. The MLEM algorithm automatically exploited this information, because it imposed non-negativity, and can therefore only explain zero line integrals by assuming an intensity of zero everywhere along the line. This resulted in an exact reconstruction of the background inside the interior region. As shown in [3], this in turn ensured exact and stable reconstruction of the interior region.

B. Data truncation from reduced transaxial detector

As a reference, the simulations of Section III.A were repeated in the absence of motion but with detector truncation. An interior region was created (figure 4b). Very similar results were found for all reconstructions (figure 6b), compared to ones from Section III.A.

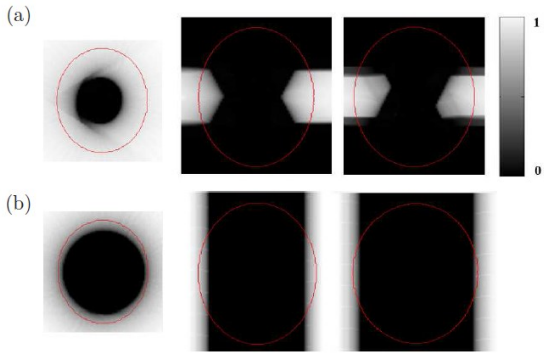

Figure 4 From left to right: coronal, sagittal and transaxial views of the Tuy map, with the contour (red) of the object in overlay, from (a) Section III.A, (b) Section III.B.

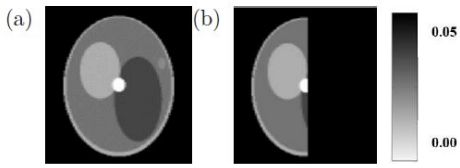

Figure 5 Coronal views of starting reference images for figure 6 with (a) full support and (b) half of the support.

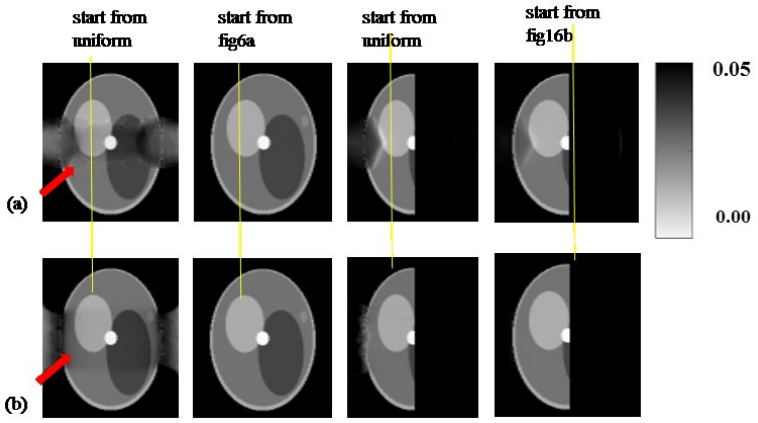

Figure 6 Coronal views (central-slice position) of reconstruction images after 1000 updates from (a) Section III.A, (b) Section III.B. Red arrow indicates the DC-shift in the interior region.

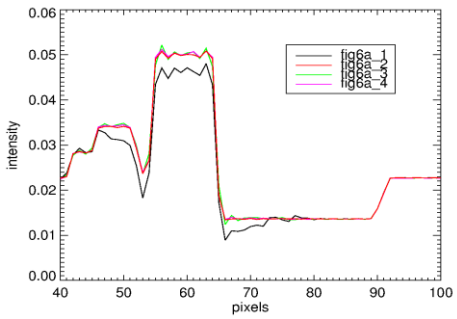

Figure 7 Profiles along the yellow lines (from left to right) in figure 6: the maximum difference between fig6a_1 and fig6a_2 is 9.6 % of the maximum intensity; the maximum difference between fig6a_3 and fig6a_4 is 0.1 %.

IV. Discussion

In our previous study [1], the Tuy value was proven to be an indicator to the risk of artefacts at a region of high Tuy values. However, it is complicated to interpret a value of zero for the local Tuy condition. This means, in the situation where the scan produces regions with increased Tuy values, we cannot conclude that exact reconstruction is possible in the region of low Tuy values. In particular, for our example of the interior-like problem, we observed that the reconstruction problem did not have a unique solution inside the interior region, unless a prior information was known inside the interior region.

In all the simulations there was a small geometric mismatch during the simulation to avoid the inverse crime. Otherwise the simulation was ideal: noise, scatter, beam hardening, etc. were not simulated, because we wanted to focus on data-insufficiency, avoiding all confounding sources of artefacts. An expectation maximization reconstruction was chosen as the reconstruction algorithm (MLEM), which is acceptable since the data were noise-free. We also tested all the simulations with another iterative algorithm, i.e. MLTR. The results were similar compared to those from III.

V. Conclusion

Although the Tuy map provides a voxel-based data-insufficiency measure, it only predicts artefact-free reconstruction when the Tuy values are low everywhere. A general theory is still warranted to summarize all the potential effects of the data-insufficiency on the reconstructed image quality.

References

[1] T. Sun, R. Clackdoyle, R. Fulton, and J. Nuyts, "Quantification of Local Reconstruction Accuracy for Helical CT with Motion Correction," in *2014 IEEE Nucl. Sci. Symp. Conf. Rec.*, 2014.

[2] F. Natterer, *The Mathematics of Computerized Tomography*. Philadelphia, PA, USA: Society for Industrial and Applied Mathematics, 2001.

[3] M. Defrise, F. Noo, R. Clackdoyle, and H. Kudo, "Truncated Hilbert transform and image reconstruction from limited tomographic data," *Inverse Probl.*, vol. 22, no. 3, pp. 1037–1053, Jun. 2006.

[4] H. Kudo, M. Courdurier, F. Noo, and M. Defrise, "Tiny a priori knowledge solves the interior problem in computed tomography.," *Phys. Med. Biol.*, vol. 53, no. 9, pp. 2207–31, May 2008.

[5] M. Courdurier, F. Noo, M. Defrise, and H. Kudo, "Solving the interior problem of computed tomography using a prior knowledge," *Inverse Probl.*, vol. 24, no. 6, p. 065001, 2008.

[6] Y. Ye, H. Yu, and G. Wang, "Exact interior reconstruction with cone-beam CT," *Int. J. Biomed. Imaging*, vol. 2007, no. 1, pp. 1–5, 2007.

[7] J.-H. Kim, J. Nuyts, A. Kyme, Z. Kuncic, and R. Fulton, "A rigid motion correction method for helical computed tomography (CT).," *Phys. Med. Biol.*, vol. 60, no. 5, pp. 2047–73, Mar. 2015.

[8] L. Shepp and Y. Vardi, "Maximum likelihood reconstruction for emission tomography.," *IEEE Trans. Med. Imaging*, vol. 1, no. 2, pp. 113–122, 1982.

[9] H. M. Hudson and R. S. Larkin, "Ordered subsets of projection data," *IEEE Trans. Med. Imaging*, vol. 13, no. 4, pp. 601–609, 1994.

[10] B. De Man and S. Basu, "Distance-driven projection and backprojection in three dimensions," *Phys. Med. Biol.*, vol. 49, no. 11, pp. 2463–2475, Jun. 2004.

[11] J. Nuyts, B. De Man, P. Dupont, M. Defrise, P. Suetens, and L. Mortelmans, "Iterative reconstruction for helical CT: a simulation study.," *Phys. Med. Biol.*, vol. 43, no. 4, pp. 729–737, Apr. 1998.

[12] K. Van Slambrouck and J. Nuyts, "Metal artifact reduction in computed tomography using local models in an image block-iterative scheme.," *Med. Phys.*, vol. 39, no. 11, pp. 7080–93, Nov. 2012.